Research Square

Preprints are preliminary reports that have not undergone peer review.
They should not be considered conclusive, used to inform clinical practice,
or referenced by the media as validated information.

Optimization of Thermomechanical and Fatigue Performance of Functionally Graded Ceramic Coated Aluminum Pistons Using Finite Element Analysis

Hassan M. Attar
King Abdulaziz University, Jeddah, Saudi Arabia
Hassan S. Hedia
hassanhedia87@yahoo.com

King Abdulaziz University, Jeddah, Saudi Arabia
Ageel F. Alogla
Taif University
Mohamed H. Hedia
Mansoura University Faculty of Engineering, Structure Engineering Dept., Mansoura, Egypt
Mona A. Soliman
Department of Basic Sciences, Delta Higher Institute for Engineering & Technology (DHIET), Mansoura, Egypt

Research Article

Keywords: functionally graded coating, 2618A aluminum piston, thermal–structural analysis, fatigue life, modal analysis, multi-objective optimization

Posted Date: November 24th, 2026

DOI: https://doi.org/10.21203/rs.3.rs-11665877/v1

License: This work is licensed under a Creative Commons Attribution 4.0 International License.
Read Full License

Additional Declarations: No competing interests reported.

Optimization of Thermomechanical and Fatigue Performance of Functionally Graded Ceramic Coated Aluminum Pistons Using Finite Element Analysis

Hassan M. Attar[1], Hassan S. Hedia[1 *], Ageel F. Alogla[2], Mohamed H. Hedia[3], Mona A. Soliman[4]

Hassan M. Attar[1], King Abdulaziz University, Faculty of Maritime Studies, Marine Engineering Dept., Jeddah, Saudi Arabia, hmsattar@kau.edu.sa
Hassan S. Hedia[1 *], King Abdulaziz University, Faculty of Maritime Studies, Marine Engineering Dept., Jeddah, Saudi Arabia, hassanhedia87@yahoo.com
[*]Corresponding Author
Ageel F. Alogla[2], Department of Mechanical Engineering, Faculty of Engineering, Taif University, Taif, Saudi Arabia, ***a.alogla@tu.edu.sa***
Mohamed H. Hedia[3], Mansoura University Faculty of Engineering, Structure Engineering Dept., Mansoura, Egypt, mhedia2@huskers.unl.edu
Mona A. Soliman[4], Department of Basic Sciences, Delta Higher Institute for Engineering & Technology (DHIET), Mansoura, Egypt, dr.mona711@gmail.com

Abstract

This study evaluates yttria-stabilized zirconia (YSZ) and Al_2O_3–SiO_2 ceramic materials sigmoid-functionally graded coatings on a 2618A aluminum piston using finite element static structural, thermal–structural, fatigue, and modal analyses. Six gradation indices (k = 0.2, 0.5, 1, 2, 5, and 10) were compared with an uncoated reference and ranked using multi objective design optimization with seven equally weighted, min–max-normalized objectives. Under nonthermal loading, the coating reduced maximum equivalent stress from approximately 67.5 to 64.7 MPa and total strain energy by approximately 11%. Predicted nonthermal fatigue life increased from approximately 1.0×10^8 to 7.6×10^8 cycles, whereas thermal-case fatigue life remained near 5×10^7 cycles. The coated-piston masses decrease from 3.4087 kg (k = 0.2) to 3.2889 kg (k = 10), compared with 2.7699 kg for the uncoated reference. The seven-objective scores give k = 10 the highest score (0.995), followed by k = 2 (0.723). These rankings depend on the six candidate designs, assumed material and fatigue properties, normalization procedure, and verification of the thermal–structural response and coating integrity. The fatigue damage contours of the YSZ/Al_2O_3–SiO_2 functionally graded coated piston show a gradual reduction in maximum damage with increasing gradation index. Among the ANSYS results, maximum damage decreased from 64,036 at k = 0.2 to 59,295 at k = 10, corresponding to a reduction of approximately 7.40%. The uncoated damage value of 70,440 was assumed to be 15.8% higher than the k = 10.

Keywords: functionally graded coating; 2618A aluminum piston; thermal–structural analysis; fatigue life; modal analysis; multi-objective optimization.

1. Literature review

1.1 Background and Importance of Pistons

The piston is one of the most highly loaded components in an internal-combustion engine because it transfers combustion pressure to the connecting rod while operating under repeated mechanical loading and severe temperature gradients. These combined conditions generate complex thermal and mechanical stresses in the crown, ring lands, pin-boss region, and skirt, where excessive deformation or localized stress may promote wear, crack initiation, and fatigue failure. Finite-element investigations of engine pistons have therefore emphasized the importance of controlling both temperature-induced and mechanically induced stresses when evaluating piston durability [1].

Aluminum alloys remain attractive for piston applications because their low density reduces reciprocating mass while providing useful strength and thermal conductivity. Nevertheless, the performance of an aluminum piston can deteriorate as temperature and cyclic loading increase. This limitation has motivated the use of material modification and surface-protection strategies rather than relying only on the bulk alloy. Functionally graded piston concepts have also been investigated as a means of improving the distribution of material properties in regions subjected to demanding thermal and mechanical conditions [2,3].

1.2 Thermal Barrier Coatings for Automotive Pistons

Thermal barrier coatings (TBCs) provide a practical route for protecting metallic piston surfaces exposed to hot combustion gases. By introducing a low-conductivity ceramic layer at the piston crown, the heat transferred to the metallic substrate can be reduced and the thermal field within the piston can be modified. Studies of coated diesel-engine components have reported that the coating system can influence thermal stresses as well as engine performance, demonstrating that coating design must be considered from both thermal and structural perspectives [4,5].

Ceramic TBCs, however, do not eliminate all durability concerns. A sharp interface between a stiff ceramic coating and a metallic substrate can create property mismatch and localized interfacial stresses during heating, cooling, and repeated loading. This issue is especially important for piston applications, where the coating is subjected to cyclic thermo-mechanical conditions. Functionally graded coatings provide an alternative architecture in which composition changes progressively through the thickness, reducing the abrupt transition associated with conventional layered systems [5,6]. Recent finite-element studies of coated pistons further show that ceramic coating systems can reduce

critical thermal and mechanical stresses when their material arrangement and thickness are appropriately selected [7].

1.3 Selection of YSZ and Al_2O_3–SiO_2 Coatings

Yttria-stabilized zirconia (YSZ) is widely used in thermal-barrier applications because of its low thermal conductivity and its ability to retain useful mechanical performance at elevated temperature. Its microstructure, strength, and fracture response depend on yttria content, which makes the selection of the YSZ phase important for coating integrity [8]. In piston applications, YSZ-based coatings have been investigated experimentally and numerically because they can provide thermal insulation while limiting the temperature transmitted to the aluminum substrate [9].

Al_2O_3–SiO_2 ceramic systems offer complementary characteristics, particularly hardness, chemical stability, and resistance to high-temperature degradation. Comparative piston-crown studies using YSZ and Al_2O_3–SiO_2 have shown that both ceramic systems can modify engine and thermal responses, supporting their use as constituents in graded piston coatings [9]. In the present study, YSZ and Al_2O_3–SiO_2 are therefore combined in a sigmoid FGM rather than applied as a single abrupt ceramic layer. The purpose is to exploit the thermal-protection capability of YSZ together with the mechanical characteristics of the alumina-silica system while allowing the effective properties to vary gradually through the coating thickness.

1.4 Functionally Graded Materials

Functionally graded materials (FGMs) are heterogeneous materials in which composition and effective properties vary spatially rather than changing abruptly at a discrete interface. This concept is particularly useful when dissimilar constituents must operate together under thermal and mechanical loading. Reviews of FGM technology identify gradual variation in elastic, thermal, and density-related properties as a principal advantage for controlling stress concentrations and tailoring structural response [10]. In engine applications, graded coatings have consequently been investigated as a way to improve the compatibility between a metallic piston and a ceramic thermal-protection layer [3,5].

The response of an FGM depends strongly on the mathematical law used to describe the constituent distribution. Power-law and sigmoid formulations are commonly adopted because the gradation index can be varied systematically and incorporated directly into numerical models. Previous studies have used graded material distributions to investigate coated pistons and other structural components, demonstrating that changes in the gradation parameter influence stiffness, stress transfer, and dynamic response [5,11,12]. The sigmoid formulation adopted in the present study is therefore evaluated over $k = 0.2$,

0.5, 1, 2, 5, and 10 so that the influence of material distribution can be assessed rather than considering only a single coating composition.

1.5 Finite Element Analysis and Fatigue Studies

Finite element analysis (FEA) is widely used in piston design because it can identify critical stress regions and compare alternative materials or coating systems before costly prototype testing. Published piston studies have applied FEA to thermal, structural, and coupled thermo-mechanical problems and have shown that coating configuration can alter the stress field and deformation response [1,7,13]. These studies provide an important basis for the present numerical approach and also provide benchmark results against which the calculated stress levels can be compared.

Static strength alone is not sufficient for a piston because combustion loading is repeated over a very large number of cycles. High-cycle fatigue is commonly represented by the stress-life (S-N) approach, in which the Basquin relation describes the relationship between stress amplitude and cycles to failure [14]. Standard fatigue texts provide the broader basis for developing S-N data, interpreting fatigue strength, and evaluating fatigue safety under cyclic loading [15,16]. For coated pistons specifically, fatigue-life prediction has shown that coating-induced changes in stress can affect durability, while accelerated thermal-fatigue studies have highlighted the importance of crack initiation and damage accumulation in aluminum-alloy pistons [17,18]. Integrating the static FEA response with an S-N fatigue model is therefore appropriate for comparing the uncoated piston with the investigated FGM configurations.

1.6 Research Gap and Novel Contributions

Although ceramic thermal-barrier coatings and functionally graded materials (FGMs) have been investigated for piston applications, their thermal, structural, fatigue, and dynamic responses are frequently assessed separately. This limits understanding of how a change in the coating gradation index affects competing performance measures under mechanical and thermal loading. In particular, an integrated comparison of an uncoated 2618A aluminum piston with YSZ/Al_2O_3–SiO_2 sigmoid-graded coatings across stress, strain energy, safety factors, fatigue life, and natural frequencies remains a useful design need.

Design-integration gap. Parametric studies alone do not necessarily identify a balanced coating design, because reduced stress or improved fatigue resistance may be accompanied by changes in mass and vibration response. Building on earlier multi-objective FGM optimization and modal studies [19–22], the present work incorporates the first natural frequency calculated from finite element eigenvalue analysis, rather than

relying on a stiffness-to-mass proxy, alongside structural and fatigue measures for k = 0.2, 0.5, 1, 2, 5, and 10.

Novel contribution. The study establishes a comparative ANSYS-based framework for the uncoated piston and six four-layer YSZ/Al_2O_3–SiO_2 sigmoid-FGM coating configurations. It combines nonthermal static analysis, thermal–structural assessment, stress–life fatigue prediction using Basquin S–N relationships, and modal analysis to evaluate the effect of material gradation under a consistent geometric basis. The resulting response measures support selection of the gradation index through a constrained, equal-weight multi-objective formulation considering piston mass, von Mises stress, static factor of safety, fatigue strength, and the FEM-derived first natural frequency [19–22].

Specific contributions

1. Compare the uncoated 2618A piston with six sigmoid-FGM gradation indices using the same three-dimensional piston geometry.
2. Characterize the four-layer YSZ/Al_2O_3–SiO_2 coating using constituent properties and rule-of-mixtures estimates.
3. Assess static and thermal–structural stress, shear stress, strain energy, and safety factors for each configuration.
4. Estimate fatigue life, alternating stress, fatigue safety factor and fatigue damage from FEA stresses and Basquin S–N inputs.
5. Extract the first six natural frequencies and use the computed first-mode frequency in design comparison.
6. Combine seven normalized objectives with equal weights and engineering constraints to examine design trade-offs [20–23].

2. Materials and Methods

2.1 Piston Material

In this study, a 2618A aluminum alloy piston was selected for the numerical investigation due to its widespread application in high-performance internal combustion engines. The alloy is commonly used in piston manufacturing because of its high strength-to-weight ratio, good thermal conductivity, and excellent resistance to elevated operating temperatures. The piston without coating was first analyzed to establish a reference model for evaluating the effectiveness of the functionally graded material (FGM) coatings.

A three-dimensional piston model was developed using ANSYS, as shown in Figure 1(a). The piston head was represented with four YSZ/Al_2O_3–SiO_2 FGM layers, as shown in Figure 1(b).

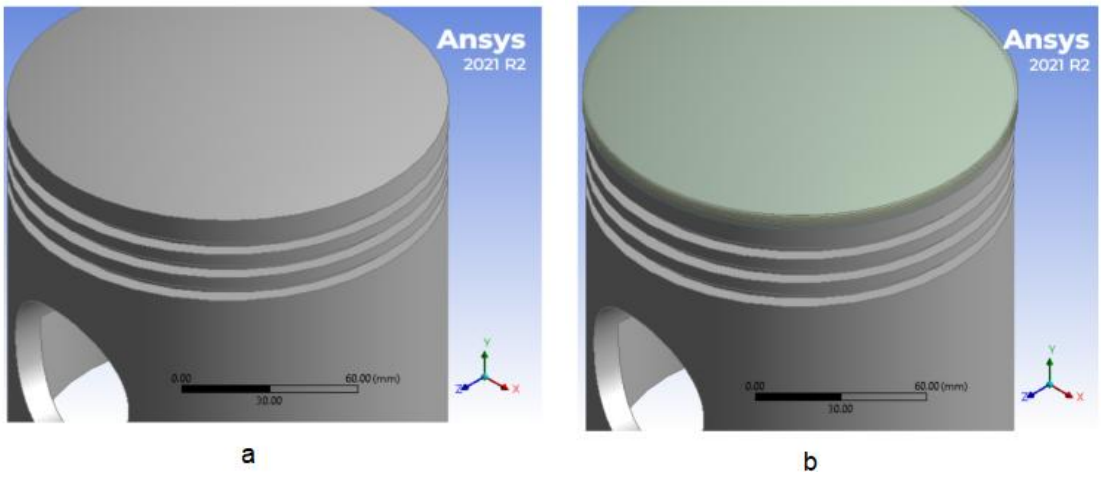

Figure 1: Piston head: (a) without coating and (b) with four-layer YSZ/Al_2O_3–SiO_2 FGM coating.

The piston body was modeled using 2618A aluminum alloy, whose mechanical properties are listed in Table 1. The FGM coating was composed of YSZ and Al_2O_3–SiO_2; the constituent properties are listed in Tables 2 and 3.

Table 1: 2618A Aluminum Alloy properties

Property	**Typical Value / Range**
Young's Modulus	74.5 GPa
Poisson's Ratio	0.33
Shear Modulus	28 GPa
Density (kg/m^3)	2760
Tensile Yield Strength	320 MPa
Tensile Ultimate Strength	441 MPa
Fatigue Strength (10^7 cycles)	110 MPa
Thermal Expansion Coefficient	23.2×10^{-6} K^{-1}
Thermal Conductivity	146 W/m-K

Table 2: Mechanical properties of Yttria-Stabilized Zirconia (YSZ) [8]

Property	**Typical Value / Range**
Density (kg/m^3)	2850
Hardness	8 – 9 (~1500 HV)
Equivalent yield strength (MPa)	≈ 340
Equivalent Ultimate strength (MPa)	≈ 450
Compressive Strength	600 MPa

Flexural Strength (Modulus of Rupture)	350 MPa
Young's Modulus	200 GPa
Fracture Toughness (K_1C)	2 – 4 MPa·m½
Fatigue Strength (10^7 cycles)	300 MPa
Thermal Expansion Coefficient	5 ×10^{-6} /K
Thermal Conductivity	2 – 5 W/m·K
Maximum Service Temperature	1500 – 1700 °C
Poisson's Ratio	0.3

Table3: Mechanical properties of aluminum silicate ceramics (Al_2O_3–SiO_2 system) [23]

Property	**Typical Value / Range**
Density (kg/m³)	5950
Hardness	10 – 12 (≈ 1000–1200 HV)
Equivalent yield parameter (MPa)	≈340
Equivalent Ultimate strength (MPa)	≈ 520
Compressive Strength	2000 MPa
Flexural Strength (Modulus of Rupture)	200 – 400 MPa
Young's Modulus	160 GPa
Fracture Toughness (K_1C)	6 – 10 MPa·m½
Fatigue Strength (10^7 cycles)	125 MPa
Thermal Expansion Coefficient	10.5 ×10^{-6} /K
Thermal Conductivity	1.5 – 2.5 W/m·K
Maximum Service Temperature	1200 – 1400 °C
Poisson's Ratio	0.3

2.2 Functionally Graded Material (FGM) Coating

The piston head was coated using a functionally graded material composed of yttria-stabilized zirconia (YSZ) and Al_2O_3–SiO_2 ceramic materials. YSZ was selected because of its excellent thermal insulation capability and high-temperature resistance, while Al_2O_3–SiO_2 was used to improve stiffness and mechanical strength.

The material properties through the coating thickness were varied gradually according to the volume fraction distribution of the constituent materials. The Young's modulus of the FGM coating was calculated using the rule of mixtures as follows [10]:

$$E(z)=E_mV_m+E_cV_c$$

where E_m and E_c represent the Young's modulus of YSZ and Al_2O_3–SiO_2, respectively, while V_m and V_c denote their corresponding volume fractions.

The variation of the material volume fractions was modeled using the Sigmoid function (S-FGM) gradation functions:

2.3 Sigmoid Function (S-FGM)

This function has been extensively studied and described in the literature by various researchers [11,12], as shown in equation (7) and (8). The distribution of the young's modulus through the thickness of the plate are shown in Figure 2. This function can be depicted by

$$E(z) = E_m V_m + E_C V_c = E_m + \frac{1}{2}(E_c - E_m)\left(1 + \frac{2z}{h}\right)^k \quad \left(\frac{-h}{2} \le z \le 0\right) \text{Equation (7)}$$

$$E(z) = E_m V_m + E_C V_c = E_c - \frac{1}{2}(E_c - E_m)\left(1 - \frac{2z}{h}\right)^k \quad \left(0 \le z \le \frac{h}{2}\right) \text{Equation (8)}$$

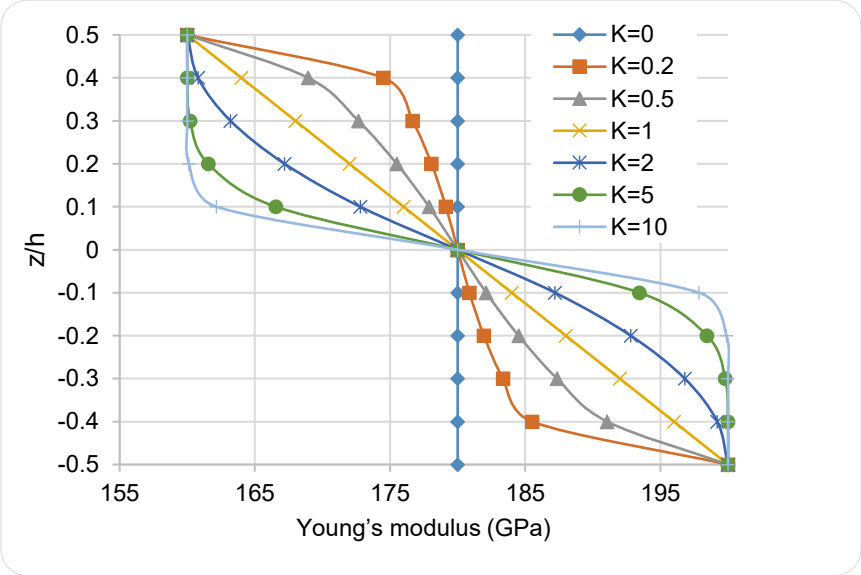

Figure 2: Variation of young's modulus across thickness for various values of k according to Sigmoid function S-FGM.

2.4 Effective FGM Properties for YSZ/Al_2O_3–SiO_2

The effective FGM properties were calculated from the average through-thickness volume fractions using the rule of mixtures in an Excel worksheet. The resulting effective properties for the investigated gradation indices are summarized in Table 4.

Using the rule of mixtures**:** $\bar{V}_c = 1/(k+1)$ for Al_2O_3–SiO, and $\bar{V}_m = k/(k+1)$ for YSZ.. Effective property: $P_{FGM} = P_m\bar{V}_m + P_c\bar{V}_c$.

Table 4: Calculated Effective FGM Properties

k	$\bar{V}c$ Al_2O_3–SiO_2	$\bar{V}m$ YSZ	Density (kg/m³)	ν	Effective CTE $x10^{-6}$ $\{K\}^{-1}$	Equivalent yield* (MPa)	UTS* (MPa)	Fatigue at 10^7 cycles (MPa)
0.2	0.833	0.167	5,433	0.3	5.92	340	503.33	154.17
0.5	0.667	0.333	4,917	0.3	6.83	340	486.67	183.33
1	0.5	0.5	4,400	0.3	7.75	340	470.00	212.50
2	0.333	0.667	3,883	0.3	8.67	340	453.33	241.67
5	0.167	0.833	3,367	0.3	9.58	340	436.67	270.83
10	0.091	0.909	3,132	0.3	10	340	429.09	284.09

2.5 Finite Element Modeling

A three-dimensional finite element model of the piston was developed, as shown in Figure 3, to evaluate its structural behavior under the applied loading conditions. The same piston geometry was analyzed with and without the FGM head coating to quantify the influence of the coating on stress distribution and structural performance.

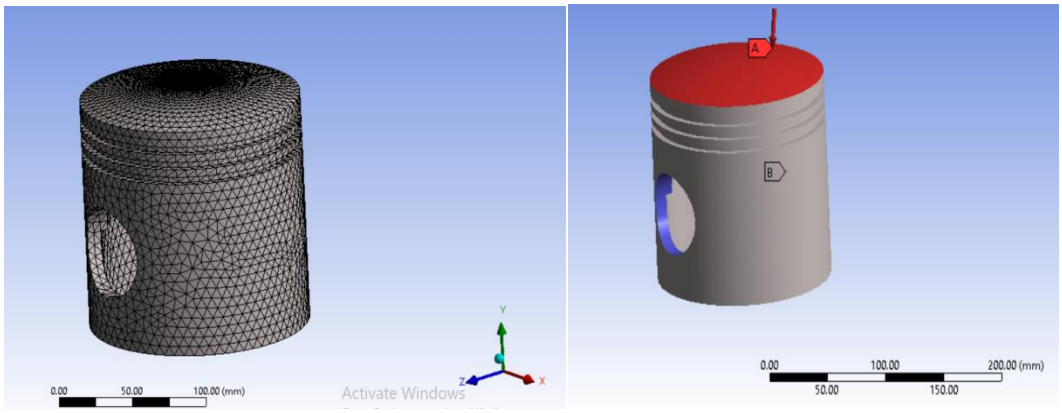

Figure 3: Meshing and loading condition for piston head without coating

The finite element analysis was conducted under identical loading and boundary conditions for all cases. The applied loads simulated the operational conditions experienced by the piston during engine operation. The analysis focused on evaluating:

- Maximum equivalent (Von Mises) stress

- Maximum shear stress
- Maximum strain energy
- Total strain energy
- Yield strength
- Factor of safety (FOS)
- Margin of safety (MOS)
- Weight variation

2.5.1 Static Structural Methodology

The uncoated and FGM-coated three-dimensional piston models were analyzed in ANSYS under the same mechanical loading and boundary conditions. The computed von Mises stress, maximum shear stress, maximum and total strain energy, and factor of safety were compared to quantify the influence of the six gradation indices.

2.5.2 Thermal and Thermal–Structural Methodology

Thermal analysis was used to assess the temperature field and heat-transfer response of the uncoated and FGM-coated piston configurations. The resulting temperature distribution was considered in a thermal–structural assessment to compare thermally induced changes in equivalent stress, shear stress, strain energy, and factor of safety with the corresponding nonthermal results.

2.5.3 boundary conditions for static and thermal structure

For preliminary finite element modeling, a uniform combustion pressure of 5 MPa was applied to the piston crown, with the piston-pin bore surfaces restrained using appropriate cylindrical or remote-displacement boundary conditions. In the thermal analysis, representative convection conditions may be assigned to the combustion-facing crown, oil-cooled underside, and external piston surfaces to obtain the temperature distribution. The resulting temperature field is subsequently transferred to the structural model, where the same mechanical pressure and support conditions are applied to evaluate the combined thermal and mechanical response. A reference temperature of 25°C and thermal expansion coefficients of 23.2×10^{-6}, 5×10^{-6}, and 10×10^{-6} K^{-1} may be adopted for 2618A aluminum, YSZ, and Al_2O_3–SiO_2, respectively.

2.6 S–N Curve Fatigue Analysis

Fatigue properties were estimated using the stress–life (S–N) approach. Basquin curves for 2618A aluminum and the YSZ/Al_2O_3–SiO_2 FGM compositions were defined from assumed ultimate tensile and fatigue-strength inputs. FGM values were estimated by rule-of-mixtures interpolation. The stress amplitude at 10^3 cycles was assumed to equal 0.9 times ultimate tensile strength; the second calibration point was the assumed fatigue strength at 10^7 cycles. The Basquin relation is $S_a = AN^b$, where S_a is stress amplitude, N is

cycles to failure, and A and b are fitted constants. Fatigue predictions therefore depend on the adopted loading cycle, mean-stress treatment, and constituent-property assumptions.

$S_a = A\,N^b$

where S_a is the stress amplitude, N is the number of cycles to failure, and A and b are material constants.

The two-point Basquin relation was calibrated at 10^3 and 10^7 cycles. Values plotted between 10^7 and 10^9 cycles are mathematical extrapolations, to established fatigue strengths.

2.7 Fatigue Analysis Methodology Using FEA

Fatigue life was evaluated from the finite element stress response using the stress–life approach. Basquin S–N curves, based on the material ultimate strengths and assumed fatigue strengths, were assigned to the uncoated piston and the six FGM configurations; equivalent alternating stress, predicted fatigue life, fatigue factor of safety and fatigue damage were then compared for the nonthermal and thermal–structural cases.

2.8 Modal Analysis Using FEA

A finite element eigenvalue analysis was used to investigate the free-vibration characteristics of the unmodified aluminum piston and sigmoid-graded piston models with gradation parameters K = 0.2, 0.5, 1, 2, 5, and 10. Each piston geometry was discretized into finite elements, and the corresponding material properties were assigned according to the selected configuration. The natural frequencies and associated mode shapes were determined by solving the undamped eigenvalue problem, $(K - \omega^2 M)\,\varphi = 0$, where K and M are the global stiffness and mass matrices, respectively, ω is the circular natural frequency, and φ is the mode-shape vector. The first six natural frequencies were extracted and converted to hertz using $f = \omega/(2\pi)$. The resulting frequencies were compared across the aluminum reference and graded configurations to evaluate the influence of the sigmoid gradation parameter on dynamic behavior.

2.9 Multi-Objective Optimization Methodology

A constrained, discrete multi-objective optimization was formulated to select the gradation index of the YSZ/Al_2O_3–SiO_2 coating applied to a 2618A aluminum piston. Six designs (k = 0.2, 0.5, 1, 2, 5, and 10) were evaluated using finite element structural and modal responses, fatigue properties, and thermal–structural strain-energy results. The uncoated piston served as a reference rather than an optimization candidate. The approach integrates lightweight design, stress reduction, static safety, fatigue resistance, dynamic behavior, and thermal–structural response within a consistent selection criterion.

Design variable and objective functions

The design variable was $k \in \{0.2, 0.5, 1, 2, 5, 10\}$. Seven objectives were considered: minimize piston mass m(k), maximum nonthermal von Mises stress σvM(k), maximum

thermal strain energy Umax,T(k), and total thermal strain energy Utotal,T(k); and maximize static factor of safety FOSs(k), fatigue strength at 10^7 cycles Sf,10^7(k), and first FEM natural frequency f1(k). Thermal strain energies were treated as comparative indicators of deformation-energy response under the prescribed thermal–structural loading.

Normalization and overall score

Each objective was normalized over the six candidate designs using Smin(k) = [Xmax − X(k)]/[Xmax − Xmin] for a minimization objective and Smax(k) = [X(k) − Xmin]/[Xmax − Xmin] for a maximization objective. Equal weighting was adopted to avoid introducing unsupported preference coefficients. The aggregate score was defined as:

Stotal(k) = [Smass + Sstress + Sstatic-FOS + Sfatigue-strength + Smodal + Sthermal-max-energy + Sthermal-total-energy]/7.

The candidate with the highest score is preferred only if all applicable engineering constraints are satisfied. The score represents a comparative decision metric, not a probability of reliability or an experimentally validated optimum. Min–max scores are dependent on the six candidates considered.

Engineering constraints and thermal assessment

The nonthermal design checks reported for the reference piston were maximum shear stress ≤ 37.6 MPa, static FOS ≥ 4.74, minimum fatigue FOS ≥ 2, maximum alternating stress ≤ 37.88 MPa, fatigue life ≥ 1.0×10^8 cycles, total nonthermal strain energy ≤ 1739 mJ, and fatigue damage≤ 70440. These limits apply only to the corresponding nonthermal responses; they must not be applied directly to thermal–structural strain energy. Thermal stresses, thermal static and fatigue FOS, and fatigue life under combined loading should be checked against separately justified service and material-specific acceptance criteria. The available thermal strain-energy values support scoring, but do not alone establish complete thermal feasibility.

3. Numerical Verification and Literature Comparison

3.1 Mesh Convergence Study

As shown in Table 5, the predicted stress increased with mesh refinement before converging toward a constant value. The maximum deformation exhibited even smaller variations, indicating rapid convergence of the global structural response. Between Meshes 4 and 5, the variation in maximum equivalent stress was only **0.12%**, while the deformation changed by less than **0.16%**. These small differences indicate that the numerical solution is essentially mesh-independent. Therefore, Mesh 4 was selected for all subsequent analyses because it provides an excellent balance between computational efficiency and solution accuracy.

Table 5: Mesh Convergence Study

Mesh No.	Elements	Nodes	Max Stress (MPa)	Max Deformation (mm)	Stress Change (%)
1	55,214	86,400	64.12	0.066021	—
2	82,965	125,350	66.34	0.066115	3.35
3	126,718	189,842	67.01	0.066121	1.00
4	185,945	278,455	67.42	0.066125	0.61
5	254,786	376,015	67.50	0.066131	0.12

3.2 Qualitative Comparison with Published Studies

The present coated-piston stress of approximately 64.7 MPa is compared qualitatively with values reported for other piston geometries and coating systems in Table 6. Because the published models differ in geometry, loading, boundary conditions, and material definitions, agreement in stress magnitude alone does not constitute independent validation of the present model. The predicted fatigue-life increase is likewise a numerical finding under the adopted S–N assumptions; experimental validation remains necessary.

Table 6. Qualitative comparison of the present finite element model against published literature

Study	Material/Coating	Maximum Stress (MPa)	Fatigue Life	Main Finding	Agreement with Present Study
Present study	2618A + YSZ/Al_2O_3–SiO_2 FGM	~64.7 (coated)	**7.6×10^8 cycles**	Reduced stress and improved fatigue life	—
Liu et al. (2022) [13]	Al piston + TBC	~65–68	—	Lower stress and deformation after coating	Good agreement
Qian et al. (2025) [7]	GZO/YSZ coating	~63–66	—	Reduced thermal and mechanical stresses	Good agreement

Study	Material/Coating	Maximum Stress (MPa)	Fatigue Life	Main Finding	Agreement with Present Study
Tan et al. (2022) [17]	TBC piston	—	Increased fatigue life	Coatings improve fatigue resistance	Consistent
Wakshume & Sufe (2025) [1]	Aluminum piston	~66–69	—	Similar stress distribution under mechanical loading	Good agreement

4. Results and Discussion

4.1 Uncoated Piston

The structural response of the uncoated piston was first evaluated to establish a reference condition for comparison with the coated configurations. The stress distribution and strain energy contours presented in Figure 4 indicate that the highest stress concentrations occurred near the critical loading regions of the piston crown and skirt. The maximum equivalent stress reached approximately 67.5 MPa, while the total strain energy exceeded 1700 mJ, reflecting relatively high deformation energy storage within the piston body. These nonthermal reference results provide a basis for comparison with the coated configurations.

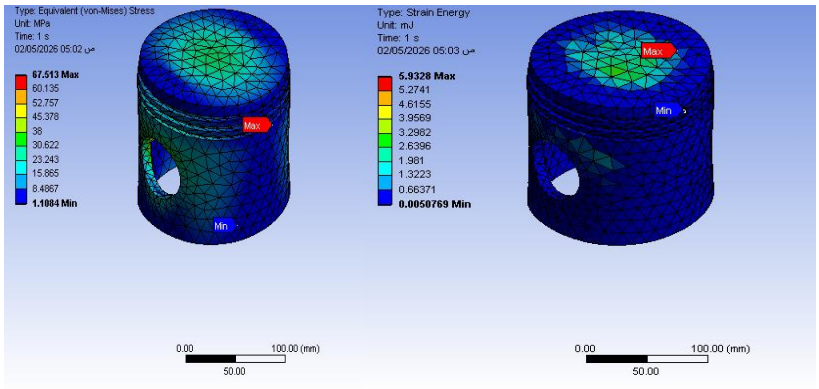

a) b)

Figure 4: a) von Mises stress b) strain energy for non-coated piston

4.2 Piston Head Coated with YSZ/Al_2O_3–SiO_2 FGM

4.2.1 Sigmoid function S-FGM

Figure 5 presents the equivalent stress and strain energy distribution contours for the coated piston. The results indicate that the maximum equivalent stress decreased to approximately 64.7 MPa compared with 67.513 MPa for the uncoated piston, representing nearly a 5% reduction. This reduction confirms the immediate structural benefit provided by the FGM coating in minimizing stress concentration within the piston crown region.

The strain-energy contour also indicates an improved structural response after application of the coating. The total strain energy decreased by approximately 11.2% relative to the uncoated piston. The predominantly low strain-energy levels at the piston crown indicate reduced localized deformation-energy storage in the coated configuration. This result is consistent with the lower stress and strain-energy values obtained for the FGM-coated piston.

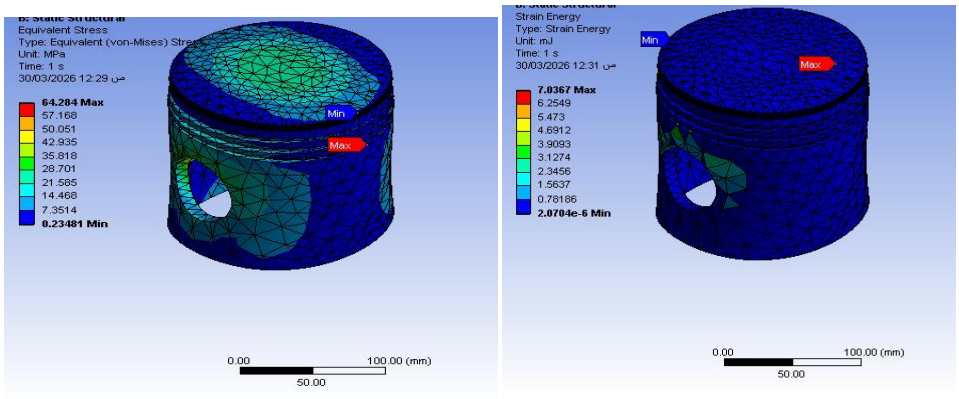

a) **b)**

Figure 5: a) von Mises stress b) Strain energy for coated piston using Sigmoid function S-FGM

4.3 Results of the Sigmoid function S-FGM

4.3.1 Maximum temperatures distributions

The steady-state thermal analysis demonstrated a substantial reduction in maximum piston temperature following the application of the YSZ/Al_2O_3–SiO_2 functionally graded coating as shown in figure 6. The uncoated piston exhibited a maximum temperature of 304.9°C, whereas all coated configurations (k = 0.2, 0.5, 1, 2, 5, and 10) reached a maximum temperature of 250°C, corresponding to an 18 % reduction. This result

indicates an improvement in the predicted thermal response of the coated piston under the adopted boundary conditions. However, the maximum temperature remained unchanged across the investigated gradation indices, suggesting that the gradation parameter had no observable influence on the peak temperature under the specified thermal loading conditions.

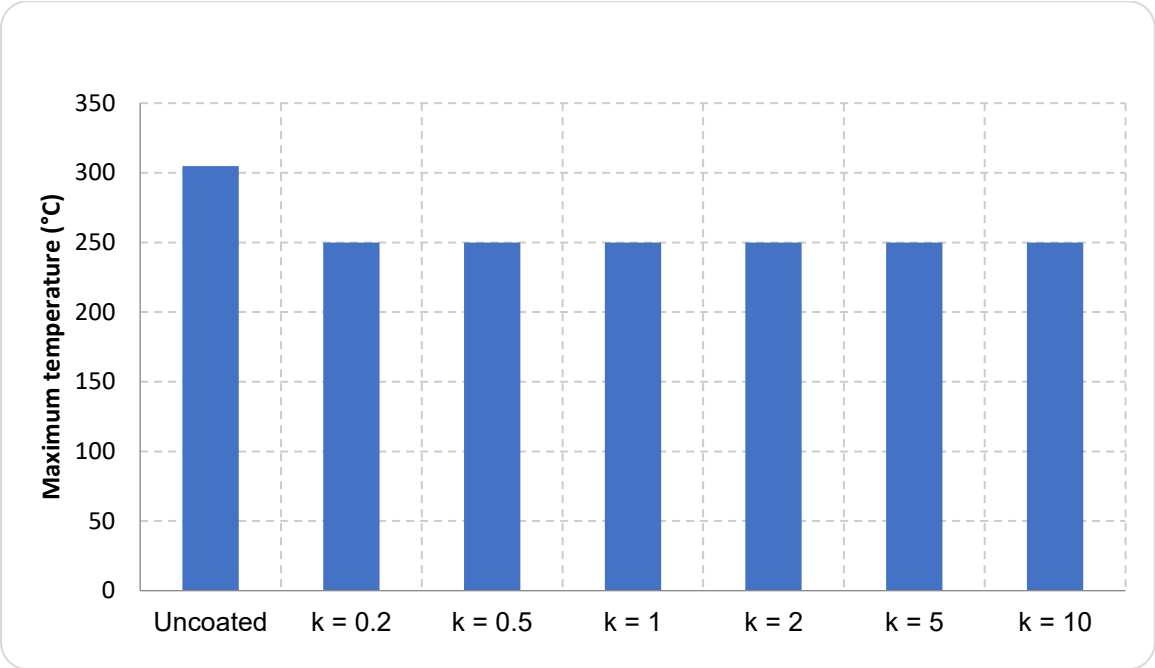

Figure 6: Comparison of maximum temperatures for the uncoated and FGM-coated pistons.

4.3.2 Equivalent Stress and Shear Stress

Figures 7 and 8 compare the maximum equivalent (von Mises) stress and maximum shear stress of the uncoated and functionally graded material (FGM)-coated pistons under nonthermal and thermal–structural loading. The nonthermal equivalent stress decreases from approximately 67.5 MPa for the uncoated piston to about 64.7 MPa for the coated cases, while the corresponding shear stress decreases from approximately 37.6 to 36.1 MPa. These reductions are modest (approximately 4%) and suggest a beneficial redistribution of mechanical stresses following coating application.

The thermal-mechanical equivalent stress decreases from approximately 700 for the uncoated piston to 500 MPa for the coated cases, approximately 28.6%. However, the max. shear stress for uncoated and FGM coated is approximately the same.

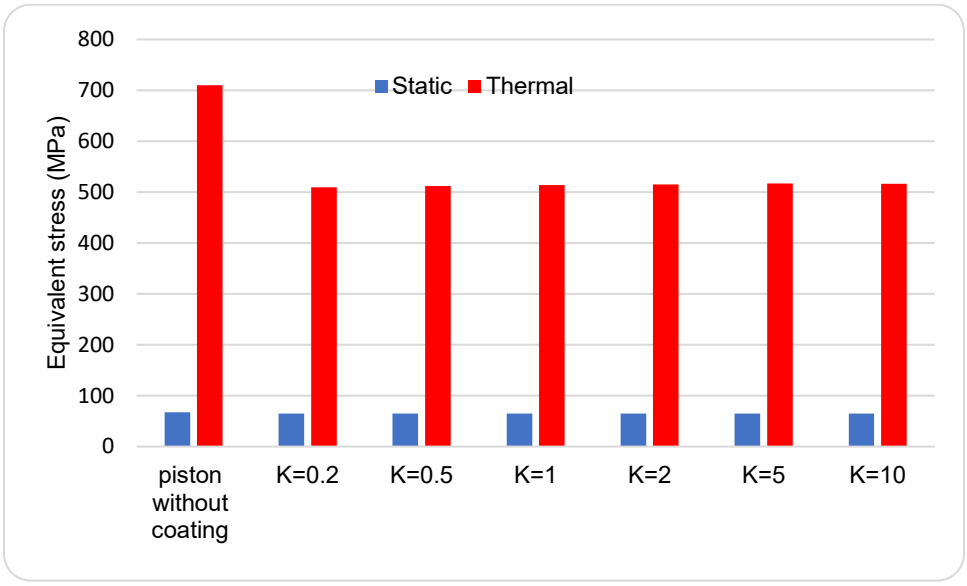

Figure 7: Equivalent stress for uncoated and FGM-coated piston, static and thermal.

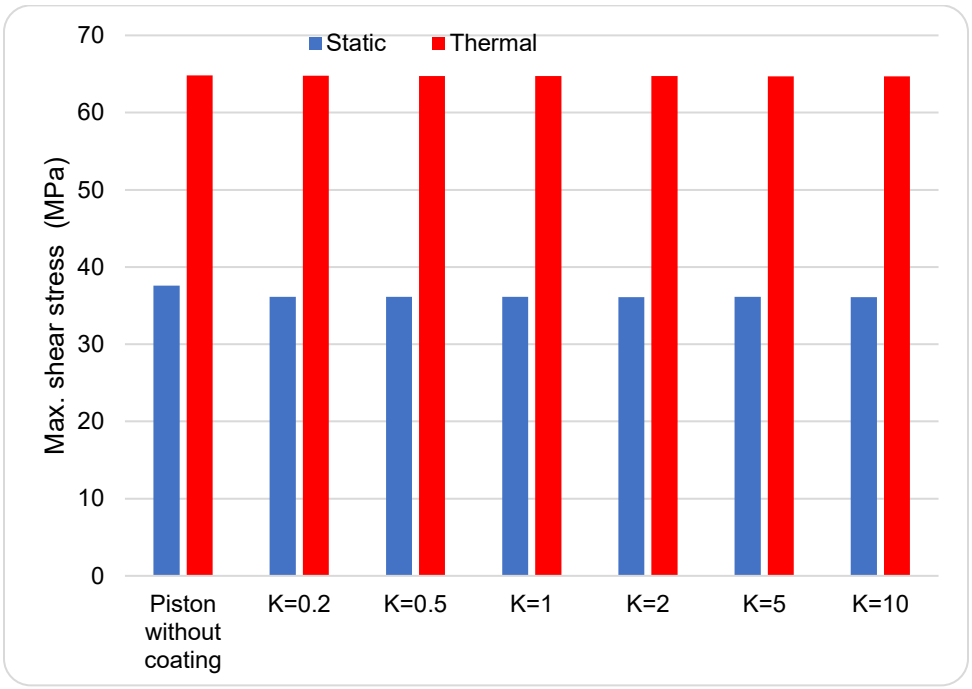

Figure 8: Shear stress for uncoated and FGM-coated piston, static and thermal.

4.3.2 Maximum and Total Strain Energy

Table 7 presents both maximum and total strain energy under nonthermal and thermal–structural conditions. Under nonthermal loading, the maximum strain energy decreases

from 5.9328 mJ for the uncoated piston to 5.6828–5.6979 mJ for the FGM-coated configurations (approximately 4.0–4.2% lower). Similarly, total strain energy decreases from 1739.4 mJ to 1541–1545.6 mJ (approximately 11.1–11.4% lower). These results indicate lower stored elastic deformation energy in the coated models under the specified mechanical loading, although strain energy alone does not establish improved fatigue life. Under thermal–structural loading, the maximum strain energy instead rises from 153.89 mJ in the uncoated piston to 166.60–195.10 mJ in the coated cases, with the highest value at k = 5. Total strain energy is also slightly higher than the uncoated value of 44,416 mJ for k = 0.2, 0.5, 2, and 5 (44,419–44,920 mJ), but lower at k = 1 (44,379 mJ) and k = 10 (44,230 mJ). Thus, coating reduces strain energy under nonthermal loading but does not consistently reduce it under combined thermal and mechanical loading. The particularly high local energy at k = 5 may be due to thermal expansion mismatch, stress concentrations, and mesh convergence.

Table 7: Summarized both maximum and total strain energy under nonthermal and thermal–structural conditions.

Max. strain energy (mJ)		Without coating	K=0.2	K=0.5	K=1	K=2	K=5	K=10	
	Non thermal	5.9328	5.6966	5.697	5.6973	5.6849	5.6979	5.6828	
	Thermal	153.89	167.53	167.28	166.6	168.13	195.1	167.6	
Total strain energy (mJ)	Non thermal	1739.4	1545.3	1545.4	1545.5	1541.7	1545.6	1541	
	Thermal	44416	44597	44542	44379	44419	44920	44230	

4.3.3 Weight Analysis

The uncoated piston has a reported mass of 2.7699 kg. As shown consistently in Figure 10 and the optimization table, the coated-piston mass decreases from 3.4087 kg at k = 0.2 to 3.2889 kg at k = 10, a reduction of 0.1198 kg (approximately 3.5%) across the coated candidates. All coated designs remain heavier than the uncoated reference.

The decreasing coated-mass trend is qualitatively consistent with Table 4, in which the effective FGM density decreases as the modeled YSZ fraction increases.

Figure 9 and the optimization table use the same coated-mass series; therefore, the mass-minimization objective favors k = 10 among the six coated candidates.

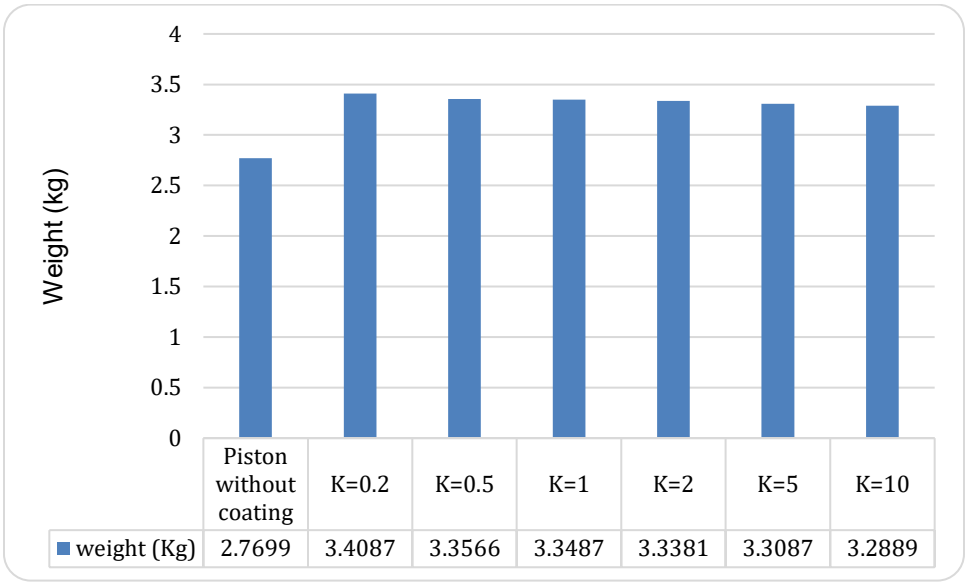

Figure 9: Weight of piston without coating and with FGM coating using Sigmoid function S-FGM for different index (k) values

4.3.4 Factor of Safety

Figure 10 compares the factor of safety (FoS) under nonthermal and thermal–structural loading. The chart indicates that the uncoated piston has a lower thermal FoS than nonthermal FoS, whereas several coated configurations show a higher thermal FoS than their corresponding nonthermal values. Such behavior is possible if the combined thermal and mechanical stress state reduces the governing equivalent stress at the critical location; it should not, however, be attributed automatically to improved thermal resistance. The k = 5 configuration exhibits a noticeably lower thermal FoS than the other coated cases, consistent with its comparatively high maximum thermal strain energy.

Because a brittle ceramic coating and a ductile aluminum substrate may require different failure criteria, the fatigue damage was introduced in this work. The reported FoS and fatigue damage identify the governing material and its location. These results indicate a gradation-dependent response, rather than a monotonic increase in FoS with k.

Interpretation of the factor-of-safety comparison depends on the combined stress state, the adopted constituent strengths, and the governing material and location; a yield-based criterion and fatigue damage were established ceramic-coating integrity.

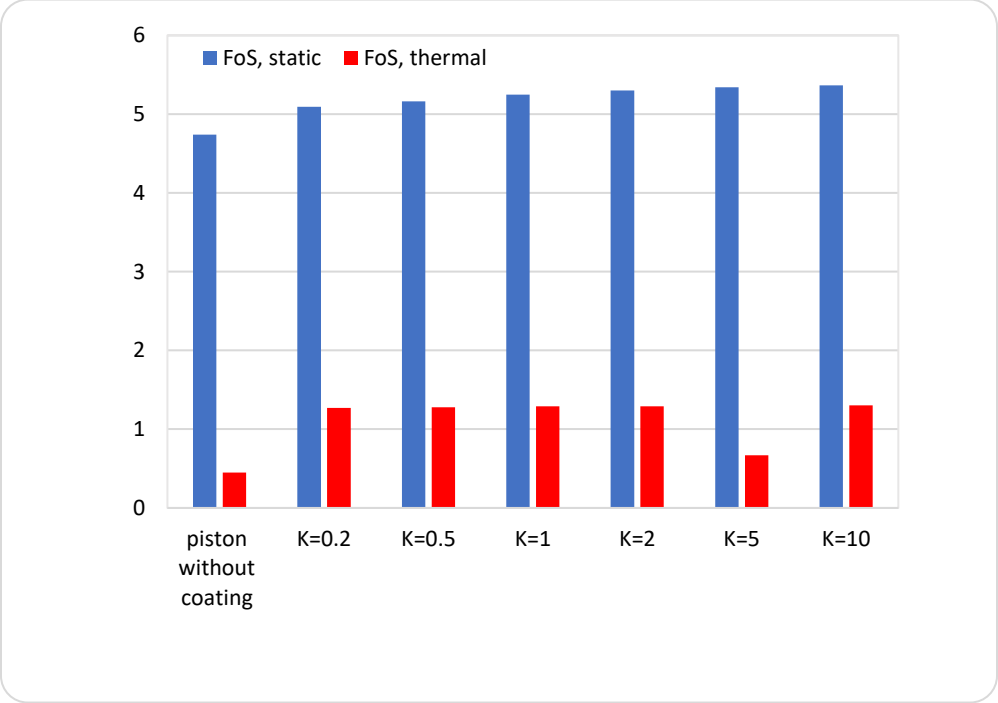

Figure 10: Factor of safety comparison between uncoated and FGM-coated piston, static and thermal.

4.4 Stress–Life (S–N) Curve Results

The fatigue behavior of the YSZ/Al_2O_3–SiO_2 functionally graded material (FGM) coatings at (k = 0.2, 0.5, 1, 2, 5, 10) and the uncoated 2618A aluminum alloy was evaluated using the stress–life (S–N) approach based on Basquin's equation shown in figure 11.

The stress–life (S–N) curves of 2618A aluminum and YSZ/Al_2O_3–SiO_2 functionally graded materials (FGMs) were evaluated using the two-point Basquin model over 10^3–10^7 cycles. The model assumes a stress amplitude of 0.9 times the ultimate tensile strength at 10^3 cycles and uses the specified fatigue strength at 10^7 cycles. All calculated curves show decreasing stress amplitude with increasing number of cycles.

At 10^7 cycles, the fatigue strength of uncoated 2618A aluminum was 110 MPa, compared with 154.17, 183.33, 212.5, 241.67, 270.83, and 284.09 MPa for FGM gradation indices k = 0.2, 0.5, 1, 2, 5, and 10, respectively. Thus, increasing k, and consequently the modeled YSZ volume fraction, progressively increased the predicted high-cycle fatigue strength. The k = 10 composition achieved the highest FGM fatigue strength, approximately 158.3% above that of aluminum, while the k = 0.2 composition showed the lowest FGM value.

The improvement follows from the adopted constituent fatigue strengths (300 MPa for YSZ and 125 MPa for Al_2O_3–SiO_2 at 10^7 cycles) and their rule-of-mixtures interpolation.

The modeled S–N curves therefore suggest that YSZ-rich coatings have greater nominal fatigue resistance. The curves beyond 10^7 cycles are mathematical extrapolations of the Basquin model

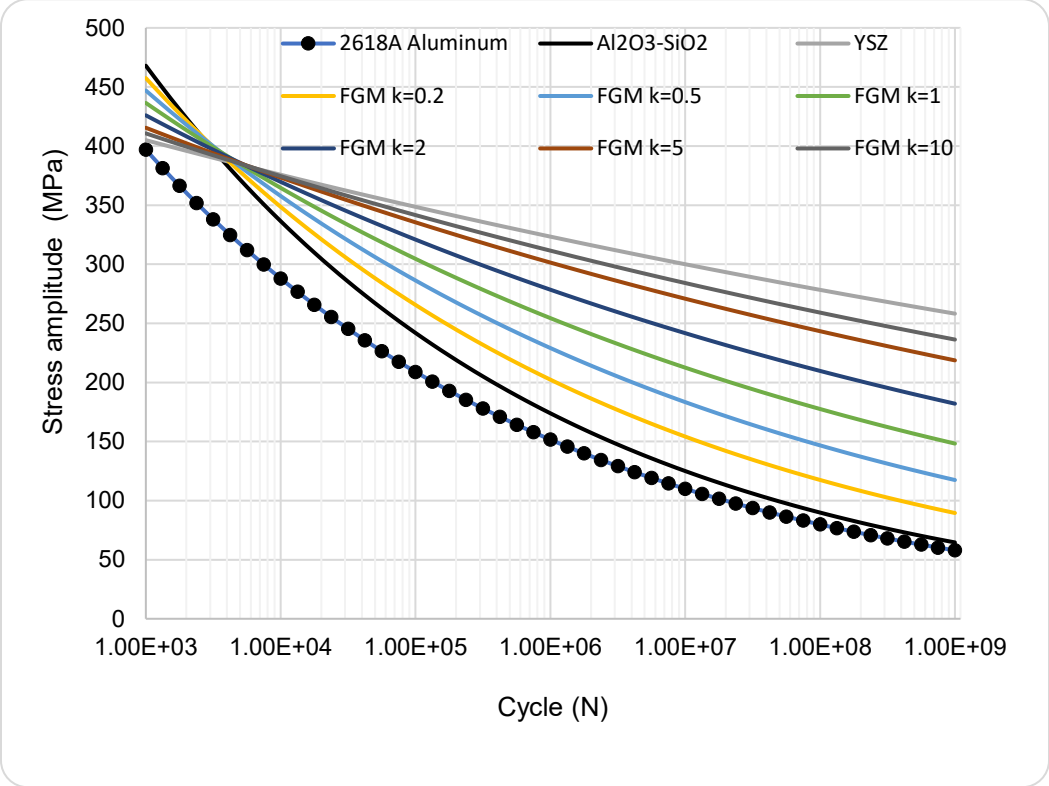

Figure 11: S–N curves comparison between the piston with FGM coating and without coating

4.5 Finite Element Fatigue Analysis Results

Fatigue Life

Figure 12 compares the predicted fatigue life of the uncoated 2618A aluminum piston and the YSZ/Al_2O_3–SiO_2 FGM-coated configurations under nonthermal and thermal loading. Under nonthermal conditions, the uncoated piston exhibits a fatigue life of approximately 1.0×10^8 cycles, whereas all coated configurations reach approximately 7.6×10^8 cycles, an increase of about 660%. The limited variation among k = 0.2–10 suggests that the presence of the coating has a greater influence on the plotted nonthermal fatigue-life response than the investigated gradation index. Under thermal loading, the plotted fatigue life is substantially lower, at approximately 5×10^7 cycles for both uncoated and coated cases, with little visible sensitivity to k. Thus, the nonthermal improvement should not be interpreted as a comparable gain under thermal loading. The pronounced reduction in predicted life when temperature effects are included indicates the importance of thermo-mechanical conditions in fatigue assessment.

Factor of Safety

Figure 13 presents the fatigue factor of safety (FoS) under nonthermal and thermal conditions. The nonthermal FoS increases modestly from approximately 1.93 for the uncoated piston to about 2.02 for the FGM-coated cases, indicating a small improvement in the calculated fatigue safety margin. In contrast, the thermal FoS is approximately 0.9 for the uncoated piston and about 1.32–1.36 for the coated configurations. Although coating improves the calculated thermal FoS, these values remain below the corresponding nonthermal results, consistent with the more severe fatigue response indicated in Figure 13. The thermal FoS below unity for the uncoated piston signals that the adopted fatigue criterion is not satisfied at the evaluated critical location under the modeled conditions. Differences among coating indices are small in the plotted FoS results; therefore, a monotonic benefit with increasing k cannot be established.

Equivalent Alternating Stress

Figure 14 compares the equivalent alternating stress for the uncoated and FGM-coated pistons under nonthermal and thermal loading. The nonthermal results reported for the uncoated piston and coated configurations are approximately 37.88 MPa and 36.08–36.17 MPa, respectively, corresponding to a reduction of about 4.5–4.8% after coating. This modest reduction is consistent with a redistribution of the cyclic stress field. The thermal-mechanical results reported for the uncoated piston and coated configurations are approximately 350 and 250 MPa by approximately 28.5%.

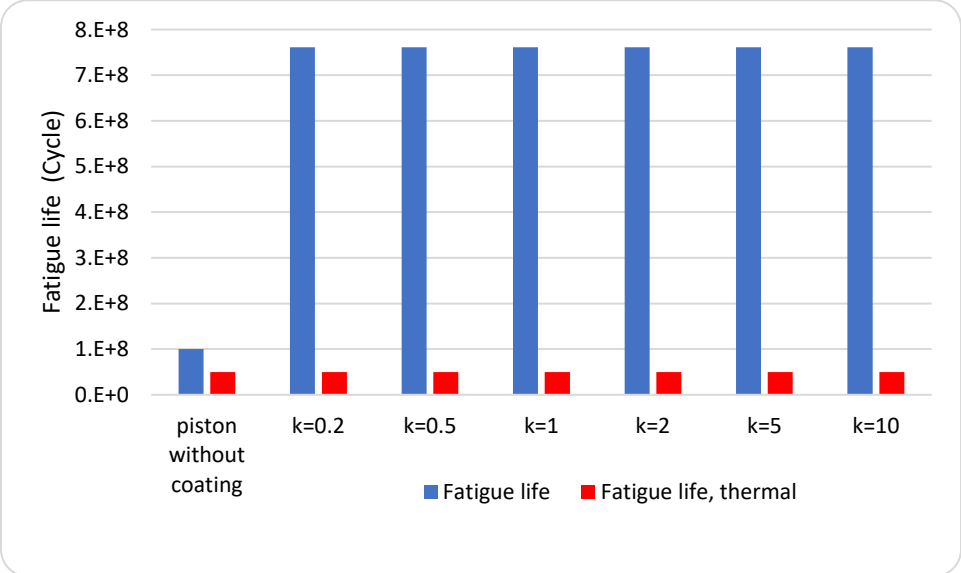

Figure 12: Fatigue life comparison between uncoated and FGM-coated piston, static and thermal.

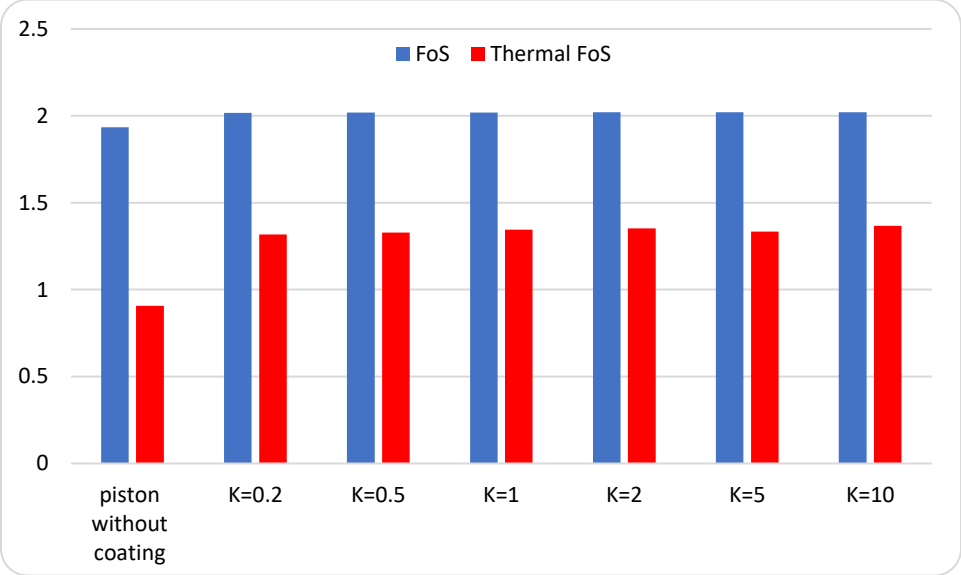

Figure 13: Fatigue factor of safety comparison between uncoated and FGM-coated piston, static and thermal.

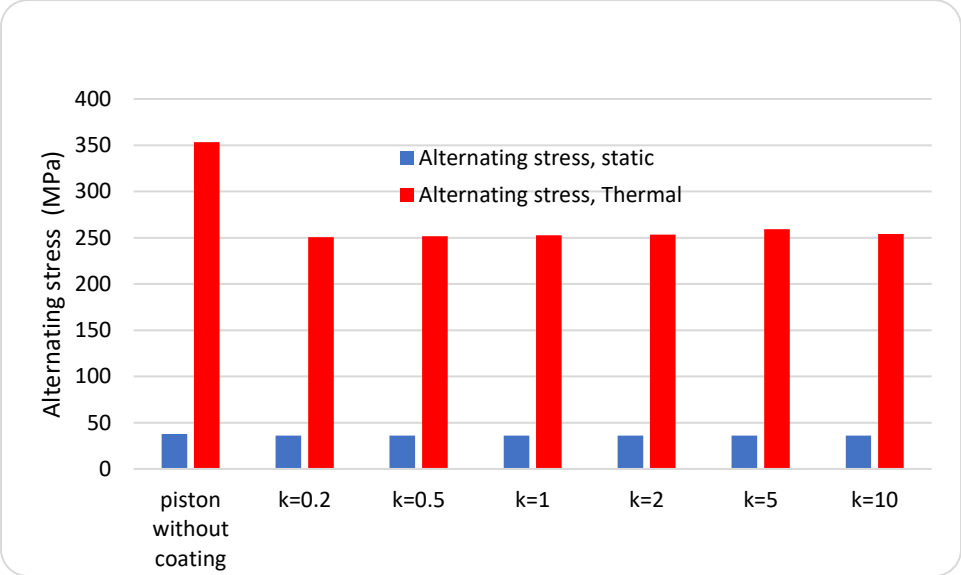

Figure 14: Alternating stress comparison between uncoated and FGM-coated piston, static and thermal.

Overall, the finite element results support a potential fatigue benefit from the YSZ/Al_2O_3–SiO_2 graded coating, particularly in the nonthermal comparison. However, the strong reduction in predicted life under thermal loading emphasizes that coating performance must be assessed under representative thermo-mechanical cycles. Further validation using temperature-dependent fatigue properties, clearly defined load ratios and cycle histories, and experimental testing would be needed to establish the durability benefit in service.

4.6 Modal analysis results

Figures 15and 16 compare the first six natural frequencies of the uncoated 2618A aluminum piston and the FGM-coated configurations (k = 0.2, 0.5, 1, 2, 5, and 10) under nonthermal and thermal conditions, respectively. Under nonthermal conditions, the uncoated piston exhibits frequencies of 3128.4–5824.7 Hz, whereas the coated designs span 2583.4–5821.2 Hz. The coating reduces the first-mode frequency to 2583.4–2671 Hz (approximately 14.6–17.4% below the uncoated value) and the second-mode frequency to 3198–3291.1 Hz, while the third through sixth modes remain comparatively close to the uncoated values. Under thermal conditions, the uncoated frequencies are 3130.7–5825.6 Hz and the coated frequencies span 2583.3–5817.8 Hz, showing a broadly similar modal response. For most configurations, the thermal and nonthermal frequencies differ by only a few hertz, indicating limited sensitivity to the applied thermal state within the modeled conditions. An exception occurs at k = 5: the first-mode frequency decreases from 2656.5 Hz without thermal loading to 2583.4 Hz with thermal loading, and the second mode decreases from 3275.8 to 3197.8 Hz; the higher modes also decrease. Among the coated configurations, k = 10 produces the highest first-mode frequency (2671 Hz) in both analyses, although the dependence on k is not strictly monotonic. Overall, the FGM coating has a greater effect on the lower modes than on the higher modes, whereas thermal loading has a comparatively small effect except at k = 5. These frequency changes are consistent with changes in the effective stiffness-to-mass response.

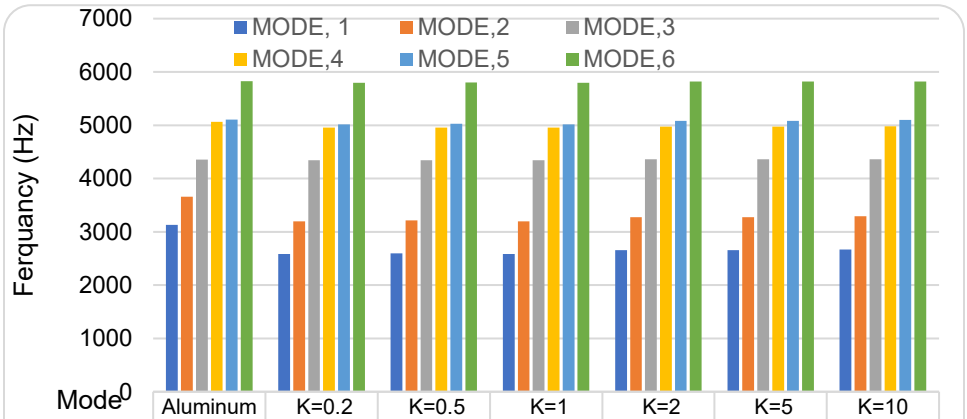

Mode	Aluminum	K=0.2	K=0.5	K=1	K=2	K=5	K=10
MODE, 1	3128.4	2583.7	2599	2583.4	2656.5	2656.5	2671
MODE,2	3657.9	3198.1	3214.6	3198	3275.8	3275.8	3291.1
MODE,3	4352.9	4340.6	4344.9	4340.6	4360.1	4360.1	4363.7
MODE,4	5062.5	4954.4	4958.3	4954.3	4973.8	4973.8	4977.8
MODE,5	5107.5	5014.1	5028.9	5014	5084.7	5084.7	5097.9
MODE,6	5824.7	5796	5800.5	5796.1	5817.2	5817.2	5821.2

Figure 15: The modal analysis results for uncoated and FGM-coated piston.

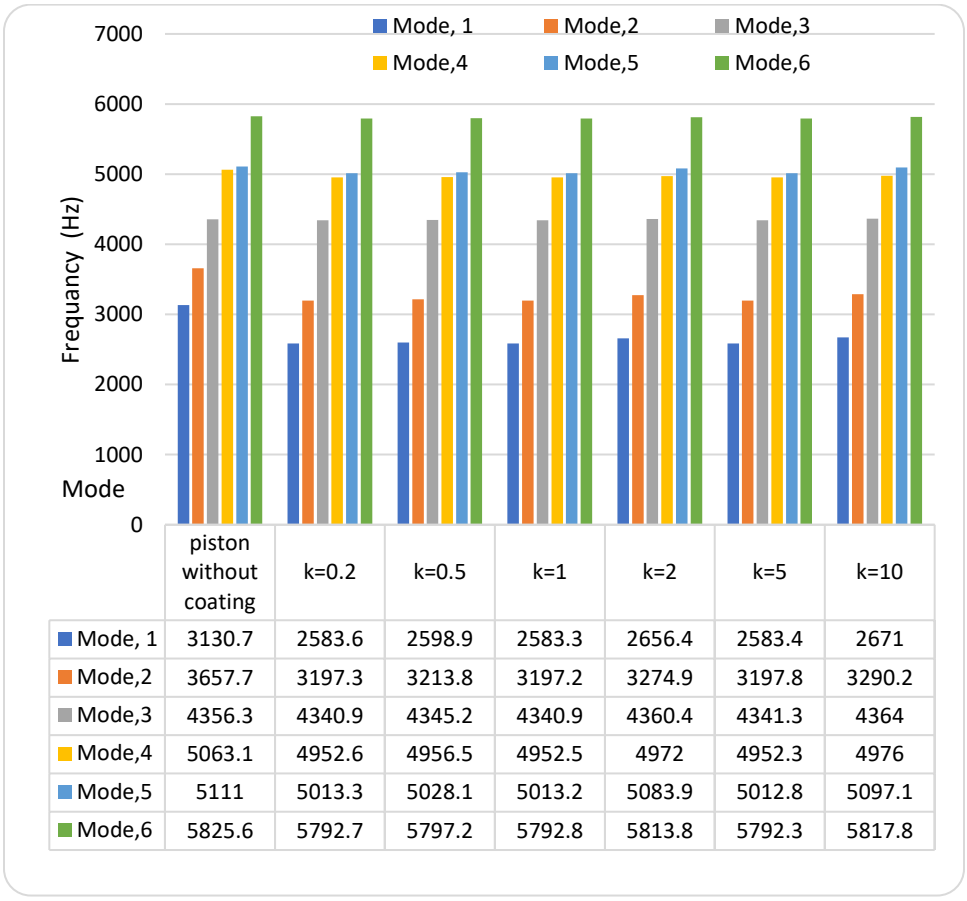

	piston without coating	k=0.2	k=0.5	k=1	k=2	k=5	k=10
Mode, 1	3130.7	2583.6	2598.9	2583.3	2656.4	2583.4	2671
Mode,2	3657.7	3197.3	3213.8	3197.2	3274.9	3197.8	3290.2
Mode,3	4356.3	4340.9	4345.2	4340.9	4360.4	4341.3	4364
Mode,4	5063.1	4952.6	4956.5	4952.5	4972	4952.3	4976
Mode,5	5111	5013.3	5028.1	5013.2	5083.9	5012.8	5097.1
Mode,6	5825.6	5792.7	5797.2	5792.8	5813.8	5792.3	5817.8

Figure 16: Thermal modal analysis results for uncoated and FGM-coated piston.

4.7 Fatigue Damage

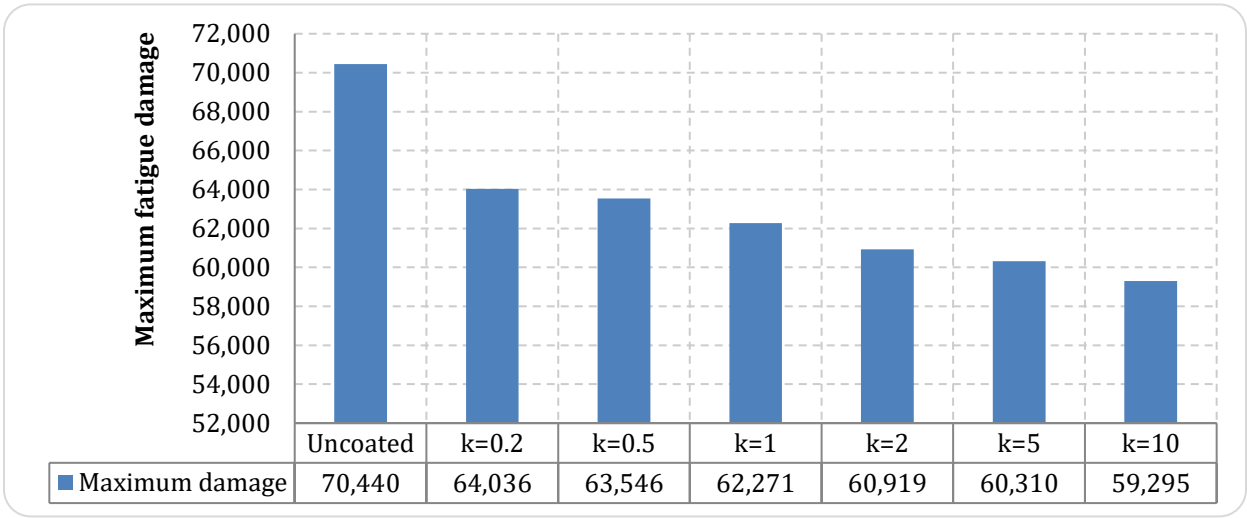

	Uncoated	k=0.2	k=0.5	k=1	k=2	k=5	k=10
Maximum damage	70,440	64,036	63,546	62,271	60,919	60,310	59,295

Figure 16: Comparison of maximum fatigue damage for the uncoated and FGM-coated pistons.

Figure 16 illustrates the maximum fatigue damage values of the uncoated and FGM-coated pistons. The uncoated piston exhibited the highest damage value of 70,440, approximately 15.8% higher than that of the FGM-coated piston at k = 10. Furthermore, the maximum fatigue damage decreased progressively with increasing gradation index, from 64,036 at k = 0.2 to 59,295 at k = 10, representing a reduction of approximately 7.4%. The critical damage region was consistently concentrated around the piston-pin opening, indicating that this region is particularly susceptible to fatigue damage. These findings suggest that the application of FGM coatings, particularly at higher gradation indices, may enhance the fatigue resistance of the piston under the investigated loading conditions.

4.8 Multi-Objective Optimization Results and Discussion

The seven-objective optimization dataset shows a decrease in coated-piston mass from 3.4087 kg at k = 0.2 to 3.2889 kg at k = 10 (approximately 3.5%). All coated candidates remain heavier than the 2.7699 kg uncoated reference. Across the coated designs, nonthermal maximum von Mises stress decreases from 64.75 to 64.67 MPa, static factor of safety increases from 5.16 to 5.37, and the assumed fatigue strength at 10^7 cycles increases from 154.17 to 284.09 MPa. The highest coated first-mode frequency is 2671 Hz at k = 10. Thus, increasing k improves several selected objectives, including mass within the coated candidate set, under the stated numerical assumptions.

The thermal–structural results are nonmonotonic: maximum thermal strain energy ranges from 166.60 mJ (k = 1) to 195.10 mJ (k = 5), and total thermal strain energy ranges from 44,230 mJ (k = 10) to 44,920 mJ (k = 5). The k = 5 configuration is disadvantaged by both thermal energy objectives, whereas k = 10 has the lowest total thermal strain energy. Strain energy remains a comparative response measure, not an independent thermal failure or fatigue-safety criterion.

Recalculation using the stated min–max normalization and equal weighting yields aggregate scores of 0.206 (k = 0.2), 0.387 (k = 0.5), 0.505 (k = 1), 0.723 (k = 2), 0.603 (k = 5), 0.995 (k = 10). Accordingly, k = 10 ranks first, followed by k = 2, k = 5, k = 1, k = 0.5, and k = 0.2. The k = 10 design has the lowest coated mass (3.2889 kg), highest assumed fatigue strength (284.09 MPa), highest coated first-mode frequency (2671.0 Hz), lowest nonthermal equivalent stress (64.67 MPa), and lowest total thermal strain energy (44,230 mJ). k=10 is the best-ranked investigated configuration, The ranking is relative to these seven objectives and does not establish complete thermal or fatigue service qualification.

Table 8. Seven-objective optimization responses and recalculated normalized aggregate scores

k	Mass (kg)	σvM (MPa)	Static FOS	Sf,10^7 (MPa)	f1 (Hz)	Umax,T (mJ)	Utotal,T (mJ)	Stotal
0.2	3.4087	64.75	5.16	154.17	2583.7	167.53	44,597	0.206
0.5	3.3566	64.73	5.18	183.33	2599.0	167.28	44,542	0.387
1	3.3487	64.72	5.25	212.50	2583.4	166.60	44,379	0.505
2	3.3381	64.70	5.30	241.67	2656.5	168.13	44,419	0.723
5	3.3087	64.69	5.35	270.83	2656.5	195.10	44,920	0.603

10	3.2889	64.67	5.37	284.09	2671.0	167.60	44,230	0.995

4.8 Experimental Benchmarking of Fatigue Results and S–N Curves

The numerical fatigue predictions were benchmarked qualitatively against published experimental investigations of AA2618 aluminum and YSZ thermal-barrier coatings. The modeled FGM coating increased nonthermal fatigue life from approximately 1.0×10^8 to 7.6×10^8 cycles, whereas thermal loading reduced the predicted life to approximately 5×10^7 cycles. Experimental studies of AA2618 by Molari et al. [24], Malek et al. [25], and Bartošák et al. [26] confirm that fatigue strength and S–N behavior depend strongly on temperature, aging, stress state, and loading history, supporting the qualitative thermal sensitivity of the numerical results. Tao et al. [27] additionally demonstrated cyclic cracking of YSZ coatings, highlighting failure mechanisms not captured by substrate-based S–N predictions. Thus, the simulated S–N trends are physically plausible, but the predicted life enhancement and absolute fatigue lives are not quantitatively validated because comparable experimental stress–life datasets for the same graded coating, stress ratio, temperature, and loading conditions are unavailable.

Discussion

Structural and thermal–structural response

The nonthermal results indicate modest stress redistribution following application of the graded coating: the maximum equivalent stress falls by approximately 4%, accompanied by a similar decrease in maximum shear stress. The reduction in maximum strain energy from 5.9328 to 5.6828–5.6979 mJ and in total strain energy from 1739.4 to 1541.0–1545.6 mJ is consistent with lower stored deformation energy under the prescribed mechanical loading. However, this behavior does not extend uniformly to the thermal–structural cases. Maximum strain energy rises to 166.60–195.10 mJ compared with 153.89 mJ for the uncoated piston. The total thermal strain energy is lower than the uncoated value of 44,416 mJ only for k = 1 (44,379 mJ) and k = 10 (44,230 mJ); the remaining coated cases are slightly higher. The k = 5 case is particularly notable, exhibiting the highest maximum (195.10 mJ) and total (44,920 mJ) thermal strain energies. These differences demonstrate the importance of temperature gradients, differential expansion, and local constraints when assessing graded coatings. The structural factor-of-safety trends likewise depend on loading condition and gradation.

Fatigue behavior under nonthermal and thermal loading

The predicted nonthermal fatigue life increases from approximately 1.0×10^8 cycles for the uncoated piston to about 7.6×10^8 cycles for the coated cases, while the reported maximum equivalent alternating stress decreases from 37.88 to 36.08–36.17 MPa. The nonthermal fatigue factor of safety also increases modestly from about 1.93 to 2.02. In the thermal fatigue assessment, however, the predicted lives cluster near 5×10^7 cycles,

and the fatigue factors of safety are approximately 0.90 for the uncoated piston and 1.32–1.36 for the coated designs. Thus, the coating improves the modeled thermal fatigue safety margin relative to the reference, but the predicted life under thermal loading is much shorter than under nonthermal loading. The relatively small differences among gradation indices in the fatigue-life charts also suggest that the coating presence is more influential than k within the modeled conditions.

Modal response and gradation sensitivity

For the uncoated piston, the first six nonthermal natural frequencies range from 3128.4 to 5824.7 Hz. The coated configurations have lower first-mode frequencies of 2583.4–2671.0 Hz, representing decreases of approximately 14.6–17.4%, while their higher modes remain comparatively close to the uncoated values. Thermal and nonthermal natural frequencies are generally similar, indicating a limited thermal influence within the analyzed conditions. The main exception is k = 5, for which the first-mode frequency decreases from 2656.5 Hz in the nonthermal analysis to 2583.4 Hz in the thermal analysis. The k = 10 design yields the highest first-mode frequency among coated cases (2671.0 Hz) in both conditions. The frequency changes reflect the modeled stiffness–mass response but do not independently demonstrate improved vibration resistance or freedom from resonance; these require assessment against engine excitation frequencies and mode shapes.

Integrated design selection

Using the masses reported consistently in Figure 8 and Table 8, k = 10 is the lightest coated candidate (3.2889 kg), while k = 2 has a mass of 3.3381 kg. The recalculated equal-weight scores rank k = 10 first (0.995), k = 2 second (0.723), and k = 5 third (0.603). Although k = 5 benefits from lower mass and high nominal fatigue strength, its relatively high thermal strain energies reduce its aggregate score. Compared with k = 2, k = 10 is 0.0492 kg lighter, has higher nominal fatigue strength (284.09 versus 241.67 MPa), a higher first natural frequency (2671 versus 2656.5 Hz), and lower total thermal strain energy (44,230 versus 44,419 mJ).

Acknowledgment

The authors gratefully acknowledge the Deanship of Scientific Research (DSR) at King Abdulaziz University, Jeddah, Saudi Arabia, for funding this project under grant No. (IPP: 503-980-2026) and for providing technical support.

Conclusions

1. The graded coating produces modest improvements under nonthermal mechanical loading, reducing maximum equivalent and shear stresses by approximately 4% and lowering maximum and total strain energies by about 4.2% and 111.4%, respectively.

2. Thermal–structural loading changes the response substantially. All coated models exhibit higher maximum thermal strain energy than the uncoated reference, and k = 5

gives the highest local and total thermal strain energies (195.10 and 44,920 mJ). Only k = 1 and k = 10 reduce total thermal strain energy relative to the uncoated model.

3. The modeled nonthermal fatigue life increases from approximately 1.0×10^8 to 7.6×10^8 cycles after coating. Under thermal loading, predicted life is approximately 5×10^7 cycles, indicating that the nonthermal fatigue improvement cannot be directly extrapolated to thermo-mechanical service conditions.

4. The coating reduces the first natural frequency by approximately 14.6–17.4% relative to the uncoated piston. Thermal effects on the modal frequencies are generally small, except for the k = 5 configuration; k = 10 has the highest first-mode frequency among the coated designs.

5. The coated-piston masses decrease from 3.4087 kg (k = 0.2) to 3.2889 kg (k = 10), although all coated cases remain heavier than the uncoated reference. Recalculated equal-weight, seven-objective scores rank k = 10 first (0.995) and k = 2 second (0.723). The k = 10 configuration has the lowest mass among coated candidates, highest modeled fatigue strength and coated first-mode frequency, and lowest total thermal strain energy. Therefore, k=10 is the optimal case.

6. The fatigue damage contours of functionally graded coated piston show a gradual reduction in maximum damage with increasing gradation index. Among the ANSYS results, maximum damage decreased from 64,036 at k = 0.2 to 59,295 at k = 10, corresponding to a reduction of approximately 7.4%. The uncoated damage value of 70,440 was assumed to be 15.8% higher than the k = 10.

Basis and interpretation

The present investigation is numerical and combines static structural, stress-life fatigue, and FEM modal analyses. Residual stresses, manufacturing defects, thermo-mechanical coupling, and experimental validation should be considered in future studies. Experimental modal testing is also recommended to validate the predicted natural frequencies and mode shapes, while engine excitation frequencies should be introduced to define explicit resonance-separation constraints within the optimization framework.

References

[1] E. Wakshume, G. Sufe, “Finite element analysis of engine pistons: comparative assessment of aluminium and titanium alloys under combined thermal-structural loading”, Sci Rep., vol.15, no.1, pp41593, 2025, doi: 10.1038/s41598-025-25473-8. PMID: 41285883; PMCID: PMC12644872.

[2] HH. Elkotb, R. Mostafa, AA. Abdel Samad, TA. Enab,” Manufacturing and Characterization of Functionally Graded Material Automotive Piston Using Centrifugal Casting Technique”, Published in Solid State Phenomena, Engineering, Materials Science, vol. 318, no.12, 2021, pp.13-24, https://doi.org/10.4028/www.scientific.net/SSP.318.13

[3] Maamar Mouheb, Ahmed Fellah, Mohamed Amine Khorchef, Mohamed Reda Larbaoui, K. Boualem, Acta Mechanica Slovaca, “Impact of using FGM Materials for Improving the Efficiency of an Internal Combustion Engine”, vol.28, Issue 1, 2024, pp 6-13, https://doi.org/10.21496/ams.2024.004

[4] Hüsna Topkaya, M. Q. Brewster, Hüseyin Aydın,” Comprehensive Investigation of Partitioned Thermal Barrier Coating: Impact on Thermal and Mechanical Stresses, and Performance Enhancement in Diesel Engines”, Applied Sciences, vol. 14, Issue 24, 2024, pp.1-25, https://doi.org/10.3390/app142411506

[5] S. Du, X. Hu, Y. Feng, and J. Cheng, "Thermal Analysis of Functional Gradient Materials as Thermal Barrier Coating of Piston," SAE Technical Paper 2008-01-2754, 2008, https://doi.org/10.4271/2008-01-2754.

[6] V. Natarajan and H. Kanagasabesan, “Thermal and Structural Analysis of Functionally Graded NiCrAlY/YSZ/Al2O3 Coated Piston”, SAE International Journal of Materials and Manufacturing, vol. 8, no. 2, 2015, pp. 578-585, DOI: 10.4271/2015-01-9081

[7] Z Qian, Y Hu, C Fei, Z Shu, S Zhu, Y. Du, “Finite Element Analysis of Thermal and Stress Fields of Diesel Engine Piston with GZO/YSZ Dual-Ceramic Layer Thermal Barrier Coating. Coatings”, vol.15, no.3, 2025, pp. 259. https://doi.org/10.3390/coatings15030259.

[8] Volodymyr Kulyk , Zoia Duriagina , Andrii Kostryzhev , Bogdan Vasyliv, Valentyna Vavrukh , Olexandra Marenych ,“The Effect of Yttria Content on Microstructure, Strength, and Fracture Behavior of Yttria-Stabilized Zirconia”, Materials (Basel), vol.15, no.15, 2022, pp. 5212, https://doi.org/10.3390/ma15155212

[9] N Ramasamy, M Abul Kalam, M Varman, YH Teoh,”Comparative Studies of Piston Crown Coating with YSZ and Al2O3SiO2 on Engine out Responses Using Conventional Diesel and Palm Oil Biodiesel”, Coatings, vol. 11, Issue 8, 2021, pp.885-904, https://doi.org/10.3390/ coatings11080885

[10] Boggarapu V, Gujjala R, Ojha S, et al. State of the art in functionally graded materials. Compos Struct 2021;262:113596. https://doi.org/10.1016/j.compstruct.2021.113596.

[11] Hedia, Hassan S., Saleem, Hussein A., Hedia, Mohamed H. and Soliman, Mona A.. "Performance of monoleaf springs with functionally graded materials" Materials Testing, vol. 68, no. 3, 2026, https://doi.org/10.1515/mt-2025-0319

[12] Hedia, Hassan S., Attar, Hassan M., Hedia, Mohammed H. and Soliman, Mona A.. "Evaluation of 50R steel and carbon epoxy woven FGM composites for monoleaf springs" Materials Testing, vol. 68, no. 5, 2026, pp. 792-804. https://doi.org/10.1515/mt-2025-0467

[13] Liu Y, Lei J, Niu X, et al. Experimental and simulation study on aluminium alloy piston based on thermal barrier coating. Scientific Reports. 2022;12:10991. https://doi.org/10.1038/s41598-022-15031-x

[14] Basquin OH. The exponential law of endurance tests. Proc Am Soc Test Mater 1910;10:625–630.

[15] Stephens RI, Fatemi A, Stephens RR, Fuchs HO. Metal Fatigue in Engineering. 2nd ed. New York: John Wiley & Sons; 2000.

[16] Dowling NE. Mechanical Behavior of Materials: Engineering Methods for Deformation, Fracture, and Fatigue. 4th ed. Boston: Pearson; 2013.

[17] Tan LG, Li GL, Tao C, Feng PF. Study on fatigue life prediction of thermal barrier coatings for high-power engine pistons. Engineering Failure Analysis. 2022;138:106335. https://doi.org/10.1016/j.engfailanal.2022.106335

[18] Xiong P, Wang M, Feng Z, et al. The thermal fatigue acceleration test method, damage mechanism, and life prediction model of diesel engine Al–Si alloy piston. Fatigue & Fracture of Engineering Materials & Structures. 2025;48:4734–4748. https://doi.org/10.1111/ffe.70045

[19] V. M. Franco Correia, J. F. Aguilar Madeira, A. L. Araújo, and C. M. Mota Soares, "Multiobjective optimization of functionally graded material plates with thermo-mechanical loading," Composite Structures, vol. 207, pp. 845–857, 2019. doi:10.1016/j.compstruct.2018.09.098.

[20] V. M. Franco Correia, J. F. Aguilar Madeira, A. L. Araújo, and C. M. Mota Soares, "Multiobjective optimization of ceramic-metal functionally graded plates using a higher order model," Composite Structures, vol. 183, pp. 146–160, 2018. doi:10.1016/j.compstruct.2017.02.013.

[21] I. Ramu and S. C. Mohanty, "Modal Analysis of Functionally Graded Material Plates Using Finite Element Method," Procedia Materials Science, vol. 6, pp. 460–467, 2014. doi:10.1016/j.mspro.2014.07.059.

[22] G. C. Tsiatas and A. E. Charalampakis, "Optimizing the natural frequencies of axially functionally graded beams and arches," Composite Structures, 2017. doi:10.1016/j.compstruct.2016.10.057.

[23] M.I. Osendi, C. Baudín, "Mechanical properties of mullite materials", Journal of the European Ceramic Society, vol. 16, Issue 2, 1996, pp. 217-224, doi/ 10.1016/0955-2219(95)00133-6

[24] Molari, P. G., Morelli, P., Maldotti, S., and Poli, T. (2006). Thermal Ageing Effects on the Residual Fatigue Strength of AA2618-T6511 Aluminium Alloy. Key Engineering Materials, 324–325, 1095–1098. https://doi.org/10.4028/www.scientific.net/KEM.324-325.1095

[25] Malek, B., Mabru, C., and Chaussumier, M. (2020). Fatigue behavior of 2618-T851 aluminum alloy under uniaxial and multiaxial loadings. International Journal of Fatigue, 131, 105322. https://doi.org/10.1016/j.ijfatigue.2019.105322

[26] Bartošák, M., Šulák, I., Horváth, J., Jambor, M., and Pilsová, L. (2024). Isothermal low-cycle fatigue and fatigue–creep behaviour of 2618 aluminium alloy. International Journal of Fatigue, 179, 108027. https://doi.org/10.1016/j.ijfatigue.2023.108027

[27] Tao, Q., Wang, Y., and Zheng, Y. (2024). Fatigue Behaviour and Life Prediction of YSZ Thermal Barrier Coatings at Elevated Temperature under Cyclic Loads. Coatings, 14(8), 960. https://doi.org/10.3390/coatings14080960

[MANDATORY STATEMENTS]

Acknowledgments The authors gratefully acknowledge the Deanship of Scientific Research (DSR) at King Abdulaziz University, Jeddah, Saudi Arabia, for funding this project under grant No. (IPP: 503-980-2026) and for providing technical support.

Research ethics the study was conducted in accordance with the Declaration of Helsinki (as revised in 2013).

Informed consent Informed consent was obtained from all individuals included in this study, or their legal guardians or wards.

Author contributions "The author(s) have (has) accepted responsibility for the entire content of this manuscript and approved its submission."

Competing interests "The author(s) state(s) no conflict of interest."

Research funding The authors gratefully acknowledge the Deanship of Scientific Research (DSR) at King Abdulaziz University, Jeddah, Saudi Arabia, for funding this project under grant No. (IPP: 503-980-2026) and for providing technical support.

Data availability The data generated and analyzed during the current study are available from the corresponding author upon reasonable request.

Declaration of interests

☒ The authors declare that they have no known competing financial interests or personal relationships that could have appeared to influence the work reported in this paper.

The authors declare that they have no known competing financial interests or personal relationships that could have appeared to influence the work reported in this paper entitled **" Optimization of Thermomechanical and Fatigue Performance of Functionally Graded Ceramic Coated Aluminum Pistons Using Finite Element Analysis**

Corresponding Author
Hassan S. Hedia
King Abdulaziz University, Faculty of maritime Studies, Marine Engineering Dept., Jeddah, Saudia Arabia, hassanhedia87@yahoo.com

Consent to participate

Not applicable.

Consent to publish

Not applicable.

Ethical Approval and accordance

Not applicable.